

NSCAT Views Land and Ice

David G. Long

Brigham Young University Microwave Earth Remote Sensing Laboratory

459 Clyde Building, Provo, UT 84602

801-378-4383, FAX: 801-378-6586, e-mail: long@ee.byu.edu

Abstract—The NASA Scatterometer (NSCAT) is a spaceborne scatterometer which flew aboard the National Space Development Agency of Japan's ADvanced Earth Observing Satellite (ADEOS). Although the three year mission was cut short due to failure of the spacecraft solar array, NSCAT returned over 9 months of observations of the Earth. NSCAT was originally designed to measure winds over the ocean; however, it also made radar backscatter measurements over land and ice regions. An overview of NSCAT land and ice observations is presented. Using the Scatterometer Image Reconstruction with Filtering (SIRF) algorithm, dual polarization global images of the incidence angle normalized radar backscatter (denoted ' \mathcal{A} ') and the incidence angle dependence of the radar backscatter (denoted ' \mathcal{B} ') are generated. When applied to NSCAT data, images with an effective resolution of better than 8 km can be produced using SIRF. Several applications for use of NSCAT \mathcal{A} and \mathcal{B} image data in land and ice studies are described, including the use of NSCAT data for ice extent mapping and for long-term vegetation change studies by comparison to 1978 Seasat data.

INTRODUCTION

The NASA Scatterometer (NSCAT) operated from Sept. 1996 through June 1997, returning 9 months of data. The Ku-band (14 GHz) NSCAT used Doppler filtering to achieve along-beam resolution [4]. NSCAT made 25 km resolution normalized radar cross section (σ^0) measurements at three azimuth angles over a dual swath, 600 km wide swath on each side with a 400 km nadir gap. The incidence angle varied from 15° to 60° . The center antenna was dual polarized while the fore and aft antennas were vertically polarized. Global coverage was achieved approximately every two days.

While the measurement geometry was designed to for retrieving winds over the ocean, NSCAT also collected σ^0 measurements over land and ice regions. Such data can be useful in a variety of studies. In this paper a number of such applications of NSCAT observations are summarized.

SAMPLE RESULTS

To aid in studying land and ice areas, enhanced resolution images are made using the Scatterometer Image Reconstruction with Filtering (SIRF) algorithm [3]. For NSCAT, the SIRF algorithm generates images of \mathcal{A} and \mathcal{B} where $\sigma^0(\text{in dB}) = \mathcal{A} + \mathcal{B}(\theta - 40^\circ)$ on a 4.45 km resolution grid using multiple passes. \mathcal{A} is the incidence angle normalized σ^0 while \mathcal{B} is the incidence angle dependence of σ^0 . Figure 1 presents sample

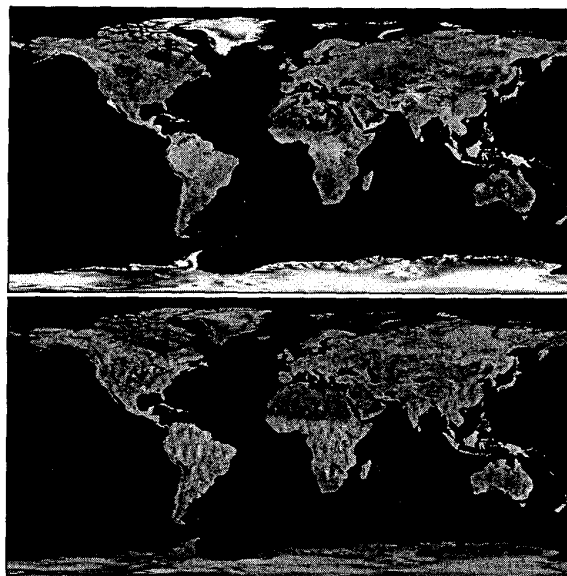


Figure 1: Top: SIRF \mathcal{A} image. NSCAT 1996 JD 320-327 v-pol data. Greyscale range is -20 to -5 dB. Bottom: \mathcal{B} image: Greyscale is -0.3 to -0.05 dB.

global \mathcal{A} and \mathcal{B} images generated by the SIRF algorithm from one week of NSCAT data. The \mathcal{A} and \mathcal{B} images correspond to the average backscatter response over the one week imaging period.

In the global images shown in Fig. 1, glacial ice exhibits the highest \mathcal{A} value followed by tropical vegetation while desert areas have a low \mathcal{A} value. \mathcal{B} is also low over desert regions and higher over tropical forests. \mathcal{B} varies significantly over ice and firn regions where it is useful in understanding the scattering mechanisms and characteristics of the snow and firn [1]. Ku-band \mathcal{A} and \mathcal{B} images have been shown to be useful for tropical vegetation classification [2] and ice facies mapping [1].

The Amazon rainforest has been used for scatterometer calibration since it is large, spatially homogeneous and temporally stable. The characteristics of the scattering can be used to accurately discriminate between different vegetation classes, including rainforest and woodlands [2]. Comparison of SASS data with NSCAT data provides a unique opportunity for observing global change in the tropical rainforest. Figure 2 shows

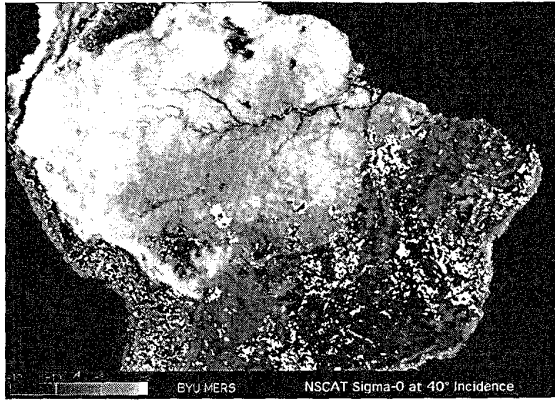


Figure 2: SIRF \mathcal{A} of the Amazon Basin. Colored patches denote areas of significant change between 1978 SASS data and 1996 NSCAT data.

regions of significant change overlaying an NSCAT SIRF image of the Amazon basin. The light region in the background image is the tropical rainforest with darker grasslands to the south. The grey mottling are areas of significant change and correspond to large-scale settlements, clearing along roads, and regions in ecological tension near forest/savannah boundaries, as well as seasonal change in the grasslands. There is clearly large areas of significant change and further analysis continues.

Increasing interest in the influence of major ice sheets upon global climate has resulted in a scientific mandate to record and monitor the extent and surface conditions of the earth's major ice bodies. Radar scatterometers offer a useful tool for the study of ice covered regions since microwave systems mitigate the need for optimal meteorological conditions and solar illumination. The wide swath of the scatterometer enables frequent, global coverage which can complement other sensors such as synthetic aperture radar.

To illustrate the temporal observation capability of the NSCAT data, even for small ice bodies, Fig. 3 presents a time series of enhanced resolution \mathcal{A} images over Iceland during late 1996. As the season progresses, liquid water in the snow cover of the ice caps (white areas in the last images) freezes, dramatically increasing \mathcal{A} as a function of time. The passage of warm fronts increases moisture in the firn, temporarily reducing \mathcal{A} . There is a general reduction in \mathcal{A} for non-glaciated regions.

Such a time-series can be effective for monitoring developments in the scattering signatures through the summer-fall transition. It is thus possible to demarcate the snow line at the end of summer, and the dry snow line at the end of the summer-fall transition [1]. While significant interannual variability in the ablation and percolation zones can be expected, the dry snow zone should change very little with time and thus should be a stable indicator of decadal change. Because SASS data was collected only in July through September, while NSCAT data

collection began in mid-September, full summer season comparisons are not yet possible. However, it is possible to gain some insight into changes in the ice sheet by comparing historic (1978) SASS data with contemporary (1996) NSCAT data.

Figure 4 shows a comparison of v-pol \mathcal{A} NSCAT and SASS images. The NSCAT image corresponds to the six day period between day 267 and 272 (24-29 Sept.) in 1996 while the SASS image corresponds to days 250 and 283 (6 Sept. - 9 Oct.) in 1978. (A longer time interval is required for SASS because of the reduced coverage of the SASS measurements relative to NSCAT.) Both images are effectively multiday averages for the time period following the autumnal freeze-up and progression of the zero degree isotherm downslope beyond the percolation zone. As evident in the difference image, there are some subtle differences between the Seasat and NSCAT images. While some of these may be related to interannual variations, some of the difference appears to be due to long term changes.

Polar sea ice is a critical component of global climate, acting as an insulating layer between the warmer ocean and cooler atmosphere and can radically change the albedo of the Earth's surface. Using the dual polarization NSCAT measurements, an automated algorithm for mapping of sea ice extent has been developed. The resulting edge closely matches the NSIDC SSM/I derived 30% ice concentration edge but has higher resolution (see Fig. 5).

CONCLUSION

Historically, spaceborne scatterometers have been employed primarily in atmospheric and oceanic studies. However, rapid repeat coverage, dual polarization, and incidence angle diversity of the NSCAT measurements make these measurements valuable in many land and ice applications where they can complement higher resolution sensors. For example, scatterometer data can be used to place SAR data into global context and supplement radiometer data.

REFERENCES

- [1] D.G. Long and M.R. Drinkwater, "Greenland Observed at High Resolution by the Seasat-A Scatterometer," *Journal of Glaciology*, Vol. 32, No. 2, pp. 213-230, 1994.
- [2] D.G. Long and P.J. Hardin, "Vegetation Studies of the Amazon Basin Using Enhanced Resolution Seasat Scatterometer Data," *IEEE Transactions on Geoscience and Remote Sensing*, Vol. 32, No. 2, pp. 449-460, Mar. 1994.
- [3] D.G. Long, P. Hardin, and P. Whiting, "Resolution Enhancement of Spaceborne Scatterometer Data," *IEEE Transactions on Geoscience and Remote Sensing*, Vol. 31, No. 3, pp. 700-715, May 1993.
- [4] F.M. Naderi, M.H. Freilich, and D.G. Long, "Spaceborne Radar Measurement of Wind Velocity Over the Ocean - An Overview of the NSCAT Scatterometer System," *Proc. IEEE*, Vol. 79, No. 6, pp. 850-866, 1991.

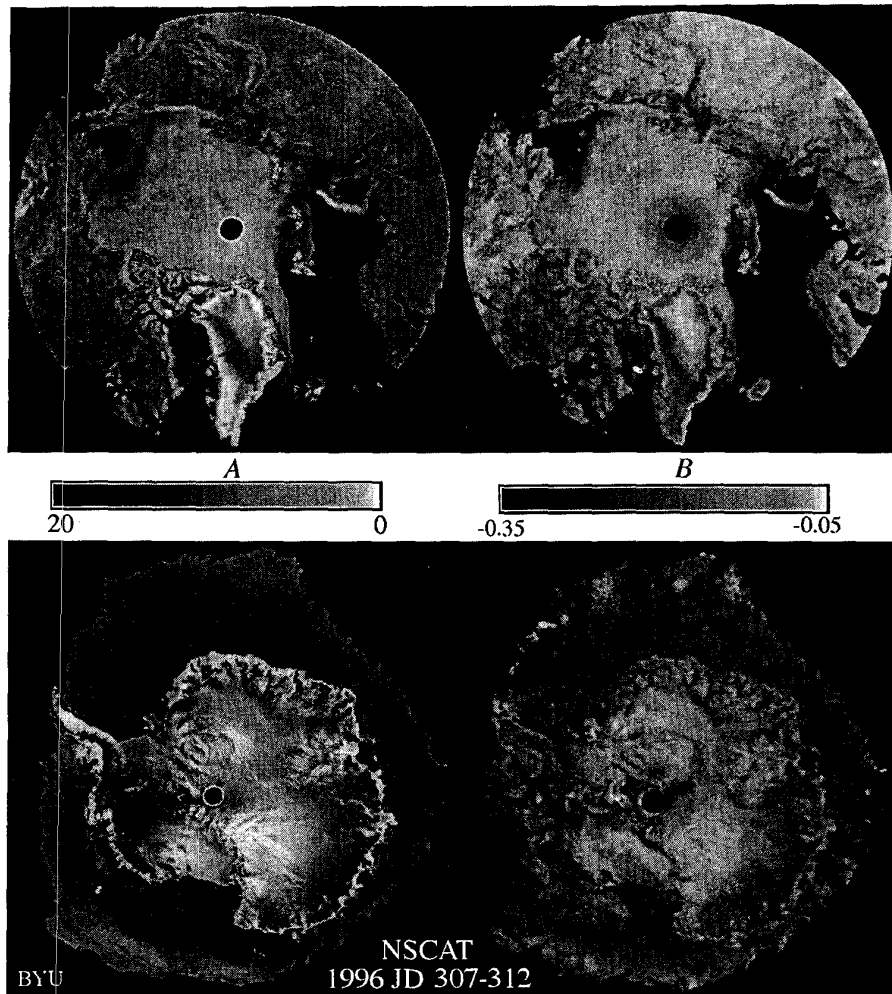


Figure 5: SIRF *A* and *B* images of the polar regions. NSCAT-derived ice mask has been applied.

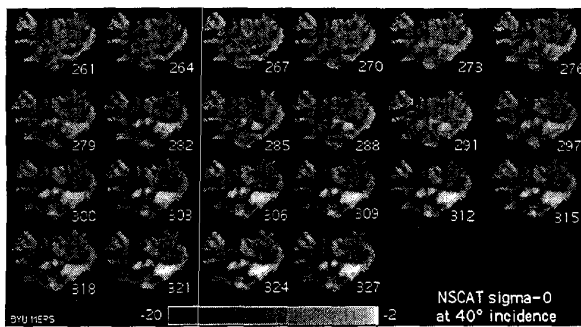


Figure 3: SIRF *A* image time series of Iceland.

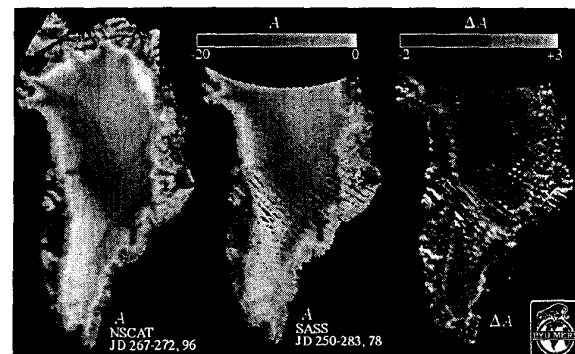


Figure 4: Comparison of 1996 NSCAT and 1978 SASS *A* images. The images and their difference are shown.